

Deuteron transverse densities in holographic QCD

Chandan Mondal^{1,2}, Dipankar Chakrabarti², and Xingbo Zhao¹

¹Institute of Modern Physics, Chinese Academy of Sciences, Lanzhou 730000, China

²Department of Physics, Indian Institute of Technology Kanpur, Kanpur-208016, India

Received: date / Revised version: date

Abstract. We investigate the transverse charge density in the longitudinally as well as transversely polarized deuteron using the recent empirical description of the deuteron electromagnetic form factors in the framework of holographic QCD. The predictions of the holographic QCD are compared with the results of a standard phenomenological parameterization. In addition, we evaluate GPDs and the gravitational form factors for the deuteron. The longitudinal momentum densities are also investigated in the transverse plane.

PACS. 13.40.Gp Electromagnetic form factors – 21.10.Ft Charge distribution – 21.45.+v Few-body systems – 25.30.Bf Elastic electron scattering

1 Introduction

The electromagnetic and gravitational form factors are among the most fundamental quantities containing information about the internal structure of the hadron. The Fourier transformation of these form factors provides information about spatial distributions such as the charge and magnetization distribution and the longitudinal momentum distribution inside the hadron. During the last decade, many experimental and theoretical investigations have been focused on deuteron in hadronic physics. For detailed reviews, see Refs. [1,2,3,4]. Since the deuteron has a spin of unity, there are three form factors, charge G_C , magnetic G_M , and quadrupole G_Q . These form factors completely describe cross sections [5,6,7,8,9,10,11,12,13,14,15,16,17] and tensor polarizations [18,19,20,21] or tensor analyzing powers [22,23,24,25,26,27] which have been probed through the electron-deuteron elastic scattering. There are many theoretical approaches such as chiral effective and phenomenological approaches, perturbative QCD, potential and quark models, holographic QCD models etc. which have been extensively used to investigate the deuteron form factors [1,2,3,4,28,29,30,31,32,33,34,35,36,37,38,39,40,41,42,43,44,45,46,47,48,49,50] whereas the generalized parton distributions (GPDs) for deuteron has been introduced in [51]. GPDs for the deuteron have been studied based on a phenomenological effective Lagrangian approach in [52]. The gravitational form factors of spin-1 particles have been evaluated using a holographic model of QCD in [53] where via sum rules, the connection of gravitational form factors to GPDs has also been established. Recently, Gutsche *et. al.* [48,49,50] have shown that the electromagnetic form factors for the deuteron in the soft-wall AdS/QCD model are well in agreement with

the experimental data and the form factors display correct $1/Q^{10}$ power scaling for large Q^2 which is consistent with the quark counting rules. Thus, it is very interesting to investigate the transverse charge densities, gravitational form factors and longitudinal momentum densities, GPDs for the deuteron in the framework of soft-wall AdS/QCD.

Recently, tremendous interests have grown in AdS/QCD formalism which emerges as one of the most promising tool to investigate the structure of hadrons. Though AdS/QCD gives only the semiclassical approximation of QCD, so far this formalism has been successfully applied to describe various hadronic properties e.g., hadron mass spectrum, parton distribution functions (PDFs), generalized parton distribution functions (GPDs), meson and nucleon form factors, transverse densities, structure functions etc. [53,54,55,56,57,58,59,60,61,62,63,64,65,66,67,68,69,70,71,72,73,74,75,76,77,78,79,80,81,82,83,84,85]. In nuclear physics, there are also some applications of holographic QCD such as holographic nuclear matter [86], ρ meson condensation at finite isospin chemical potential [87], nuclear matter to strange matter transition [88], baryon matter at finite temperature and baryon number density [89], cold nuclear matter [90], heavy atomic nuclei [91], mean-field theory for baryon many-body systems [92]. Many other interesting works have been done in nuclear physics using AdS/QCD formalism (see Refs. [93,94,95,96] for detailed reviews).

The charge densities in the transverse plane are defined as the two dimensional Fourier transforms of the charge form factors. The transverse densities are also intimately related to the GPDs with zero skewness [97,98]. Since the form factor involves initial and final states with different momenta, three dimensional Fourier transforms cannot be interpreted as densities. However, the transverse

densities defined at fixed light-front time have a proper density interpretation [99, 100, 101]. The charge densities in the transverse impact parameter plane for the nucleon have been discussed extensively in various phenomenological models [63, 64, 74, 102, 103, 104, 105, 106, 107, 108, 109], whereas the densities in the transverse coordinate plane have been studied in [110, 111, 112]. In [113], the deuteron transverse charge density has been evaluated using different parameterizations of the charge form factor and it has been shown that the different parameterizations provide different densities in particular at the center of the impact parameter ($b = 0$). The deuteron transverse charge density has been studied using the phenomenological Lagrangian approach in [114]. Using the parameterization of the deuteron form factor data [1], the transverse charge density in the deuteron has been mapped out in [115] where the authors considered both the longitudinally and transversely polarized deuteron. In a similar fashion of charge density in the transverse plane, one can map out the longitudinal momentum distribution within a hadron by taking the two dimensional Fourier transformation of the gravitational form factor [116, 104]. The longitudinal momentum distributions within nucleons based on the phenomenological parameterization of GPDs and a similar distributions for spin-1 objects using theoretical results from the AdS/QCD correspondence have been calculated in [116]. A nice comparative investigation of charge and momentum density distributions has been done in [104] where the authors used a different t -dependence of GPDs from the Ref.[116] with same quarks distributions. Using a light front quark-diquark model in AdS/QCD, the longitudinal momentum densities have been evaluated for both the unpolarized and the transversely polarized nucleons in [117, 118]. A comparative study of the longitudinal momentum distribution for the nucleon in two different soft-wall AdS/QCD has been presented in [76]. In the present paper, using the recent empirical description of the deuteron electromagnetic form factors in the framework of soft-wall AdS/QCD, we investigate the transverse charge densities within a deuteron. We consider both the longitudinally and transversely polarized deuteron. In addition, we evaluate the GPDs and gravitational form factors for the deuteron which are further used to study the longitudinal momentum densities in the transverse plane.

This paper is organized as follows. A brief description of the electromagnetic form factors of the deuteron in the soft-wall AdS/QCD model has been given in Sec.2. The charge densities in the transverse plane for both unpolarized and transversely polarized deuterons have been analyzed in Sec.3. In Sec.4, we present the deuteron GPDs and the results of gravitational form factors and the longitudinal momentum densities have been evaluated in Sec.5. Finally, we provide a brief summary in Sec.6.

2 Deuteron form factors

The matrix element which describes the interaction of the deuteron with the electromagnetic field relates three form

factors as

$$\begin{aligned} M_{\text{inv}}^\mu(p, p') = & - \left(G_1(Q^2) \epsilon^*(p') \cdot \epsilon(p) \right. \\ & - \frac{G_3(Q^2)}{2M_d^2} \epsilon^*(p') \cdot q \epsilon(p) \cdot q \left. \right) (p + p')^\mu \\ & - G_2(Q^2) \left(\epsilon^\mu(p) \epsilon^*(p') \cdot q - \epsilon^{*\mu}(p') \epsilon(p) \cdot q \right), \end{aligned} \quad (1)$$

where $G_{1,2,3}$ are the form factors; $\epsilon(\epsilon^*)$ and $p(p')$ are the polarization and four-momentum of the initial(final) deuteron, and $q = p' - p$ is the momentum transfer. The electromagnetic form factors $G_{1,2,3}$ of the deuteron are again related to the charge G_C , quadrupole G_Q and magnetic G_M form factors by

$$G_C = G_1 + \frac{2}{3}\eta G_Q, \quad (2)$$

$$G_M = G_2, \quad (3)$$

$$G_Q = G_1 - G_2 + (1 + \eta)G_3, \quad (4)$$

with $\eta = \frac{Q^2}{4M_d^2}$ and normalization $G_C(0) = 1, G_Q(0) = M_d^2 \mathcal{Q}_d = 25.83$, and $G_M(0) = \frac{M_d}{M_N} \mu_d = 1.714$, where M_d and M_N are the deuteron and nucleon masses, and $\mathcal{Q}_d = 7.3424 \text{ GeV}^{-2}$ and $\mu_d = 0.8574$ are the quadrupole and magnetic moments of the deuteron.

For the derivation of the deuteron electromagnetic form factors in the framework of soft-wall AdS/QCD we follow the works of Gutsche *et al.* [48, 49, 50]. For a hadronic bound state, the twist which is defined as dimension – spin, can also be written as $\tau = n_p$ where n_p is the number of partons in a bound state [55, 56, 57, 83]. The ground state of the deuteron which is a bound state of a proton and a neutron having six partons is described by $\tau = 6$ wavefunctions. The effective action in terms of the AdS fields $d^M(x, z)$ and $V^M(x, z)$ which are dual to the Fock component contributing to the deuteron with twist $\tau = 6$ and the electromagnetic field, respectively, is given by [48]

$$\begin{aligned} S = \int d^4x dz e^{-\varphi(z)} \left[-\frac{1}{4} F_{MN} F^{MN} - D^M d_N^\dagger D_M d^N \right. \\ - i c_2 F^{MN} d_M^\dagger d_N + \frac{c_3}{4M_d^2} e^{2A(z)} \partial^M F^{NK} \left(i D_K d_M^\dagger d_N \right. \\ \left. - d_M^\dagger i D_K d_N + \text{H.c.} \right) + d_M^\dagger \left(\mu^2 + U(z) \right) d^M \left. \right], \end{aligned} \quad (5)$$

where $A(z) = \log(R/z)$, the stress tensor: $F^{MN}(x, z) = \partial^M V^N(x, z) - \partial^N V^M(x, z)$, D^M is the covariant derivative, $\mu^2 R^2 = (\Delta - 1)(\Delta - 3)$ is the five-dimensional mass and R is the AdS radius. The background dilaton field $\varphi(z) = \kappa^2 z^2$. For a state with n_p partons and L orbital angular momentum, the scaling dimension is defined as $\Delta = n_p + L$ [55, 56, 57]. However, $n_p = \tau$ which corresponds to the fact that the dimension of the $d^M(x, z)$ field is $\Delta = \tau + L$. The first and second terms in Eq.5 correspond to kinematic parts of the electromagnetic and the deuteron fields respectively whereas the last part of the action denotes the effective mass term. The rest of the terms in the effective action is due to the interaction which are

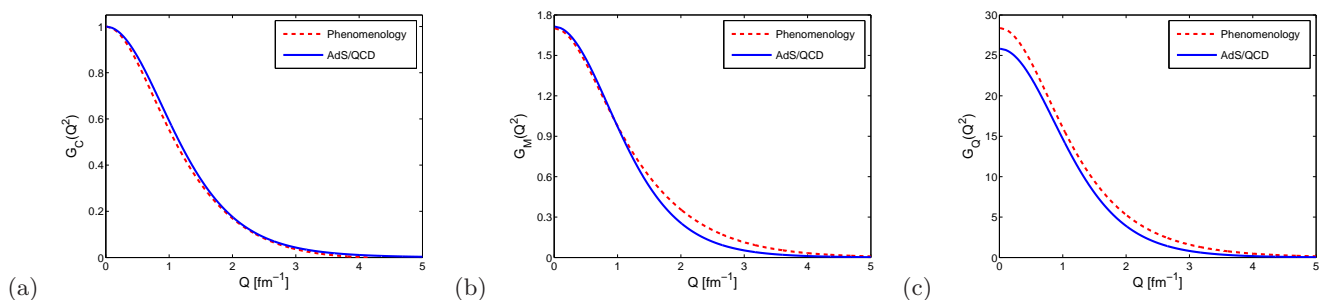


Fig. 1. (Color online) Deuteron electromagnetic form factors (a) $G_C(Q^2)$, (b) $G_M(Q^2)$ and (c) $G_Q(Q^2)$ are plotted against $Q \text{ fm}^{-1}$. The red dashed line represents the phenomenological parameterization of the deuteron form factors data [1] and the solid blue line represents the results of soft-wall AdS/QCD.

responsible for generating the deuteron form factors. The pure AdS geometry reproduces the kinematical aspects of the light-front Hamiltonian whereas the breaking of the maximal symmetry of AdS by the background dilaton field allows the confinement dynamics of the theory in physical space-time. In general, the presence of the quadratic covariant derivatives with a dilaton in the effective action leads to a mixture of kinematical and dynamical effects. The z -dependent effective mass $\mu_{eff}(z) = \mu^2 + U(z)$ is chosen to cancel the interference term and keep the mass term μ^2 independent of z [83,84]. $U(z)$ in the effective mass gives the confinement potential with $U(z) = \frac{\varphi(z)}{R^2} U_0$, where the constant U_0 is determined by the value of the deuteron mass M_d , and the parameters c_2 and c_3 are obtained by normalization of the deuteron electromagnetic form factors. Using the Kaluza-Klein decomposition for the vector AdS field dual to the deuteron

$$d^\mu(x, z) = \exp\left[\frac{\varphi(z) - A(z)}{2}\right] \sum_n d_n^\mu(x) \Phi_n(z), \quad (6)$$

where $\Phi_n(z)$ are their bulk profiles and $d_n^\mu(x)$ is the tower of the Kaluza-Klein fields dual to the deuteron fields with radial quantum number n and twist-dimension $\tau = 6$, one can derive the equation of motion for the bulk profile $\Phi_n(z)$ as [48]

$$\left[-\frac{d^2}{dz^2} + \frac{4(L+4)^2 - 1}{4z^2} + \kappa^4 z^2 + \kappa^2 U_0\right] \Phi_n(z) = M_{d,n}^2 \Phi_n(z). \quad (7)$$

This is a Schrödinger-type equation and the solutions of the Eq.(7) are given by

$$\Phi_n(z) = \sqrt{\frac{2n!}{(n+L+4)!}} \kappa^{L+5} z^{L+9/2} \times e^{-\kappa^2 z^2/2} L_n^{L+4}(\kappa^2 z^2), \quad (8)$$

$$M_{d,n}^2 = 4\kappa^2 \left[n + \frac{L+5}{2} + \frac{U_0}{4}\right], \quad (9)$$

where $L_n^m(x)$ are the generalized Laguerre polynomials. For the ground state i.e. $n = 0$, $L = 0$, one gets $M_d = 2\kappa \sqrt{\frac{5}{2} + \frac{U_0}{4}}$. Using the data for the deuteron mass $M_d =$

1.875613 GeV the scale parameter $\kappa = 190 \text{ MeV}$ which is fixed by fitting the electromagnetic form factors of the deuteron with experimental data, the constant U_0 is found to be 87.4494 [48]. In the soft-wall AdS/QCD framework, the deuteron electromagnetic form factors $G_{1,2,3}(Q^2)$ can be expressed in terms of the universal form factor $F(Q^2)$ such as [48,49]

$$G_1(Q^2) = F(Q^2), \quad (10)$$

$$G_i(Q^2) = c_i F(Q^2), \quad \{i = 2, 3\} \quad (11)$$

where $F(Q^2)$ is the twist-6 hadronic form factor, which is given by the overlap of the square of the bulk profile dual to the deuteron wave function and the confined electromagnetic current

$$F(Q^2) = \int_0^\infty dz \Phi_0^2(z) V(Q, z). \quad (12)$$

$V(Q, z)$ is the vector bulk-to-boundary propagator dual to the $Q^2 (= -q^2)$ -dependent electromagnetic current and the integral representation of $V(Q, z)$ is given by [67,68],

$$V(Q, z) = \kappa^2 z^2 \int_0^1 \frac{dx}{(1-x)^2} e^{-\kappa^2 z^2 x/(1-x)} x^a. \quad (13)$$

Using the deuteron wave function $\Phi_0(z)$ from Eq.(8) and $V(Q, z)$ from Eq.(13), one finds $F(Q^2)$ as

$$F(Q^2) = \frac{\Gamma(6) \Gamma(a+1)}{\Gamma(a+6)}, \quad (14)$$

with $a = Q^2/(4\kappa^2)$. Note that the formula follows the the general form of the hadronic form factor with twist τ : $F_\tau(Q^2) = \frac{\Gamma(\tau) \Gamma(a+1)}{\Gamma(a+\tau)}$ derived in [57]. The parameters c_2 and c_3 in Eq.(11) are determined by the normalization of the deuteron form factors as defined in [48]: $c_2 = G_M(0) = 1.714$, and $c_3 = G_M(0) + G_Q(0) - 1 = 26.544$. We show the deuteron electromagnetic form factors $G_C(Q^2)$, $G_M(Q^2)$ and $G_Q(Q^2)$ obtained in the soft-wall the AdS/QCD model in Fig.1. The results are compared with the phenomenological parameterization of the

experimental data of the deuteron form factors [1]. One observes that G_C evaluated in AdS/QCD framework are in excellent agreement with the parameterization and G_M and G_Q in soft-wall AdS/QCD model are also in more or less agreement with the parameterization.

3 Transverse charge densities in the deuteron

According to the standard interpretation [102,103,104,109,74], the charge density in the transverse plane can be identified with the two-dimensional Fourier transform (FT) of the electromagnetic form factors in the light-cone frame with $q^+ = q^0 + q^3 = 0$. Thus, the transverse charge densities for the deuteron in helicity states of $\lambda = \pm 1$ or $\lambda = 0$ are defined as,

$$\begin{aligned} \rho_\lambda^d(b) &\equiv \int \frac{d^2 \mathbf{q}_\perp}{(2\pi)^2} e^{-i \mathbf{q}_\perp \cdot \mathbf{b}_\perp} G_{\lambda\lambda}^+(Q^2) \\ &= \int_0^\infty \frac{dQ}{2\pi} Q J_0(bQ) G_{\lambda\lambda}^+(Q^2), \end{aligned} \quad (15)$$

where the form factor $G_{\lambda\lambda'}^+(Q^2)$ is again related to the matrix elements of the electromagnetic current $J^+(0)$ operator between deuteron states as,

$$\begin{aligned} &\langle P^+, \frac{\mathbf{q}_\perp}{2}, \lambda' | J^+(0) | P^+, -\frac{\mathbf{q}_\perp}{2}, \lambda \rangle \\ &= (2P^+) e^{i(\lambda - \lambda')\phi_q} G_{\lambda'\lambda}^+(Q^2), \end{aligned} \quad (16)$$

with $\lambda = \pm 1, 0$ ($\lambda' = \pm 1, 0$) which denotes the initial (final) deuteron light-front helicity, and $\mathbf{q}_\perp = Q(\cos \phi_q \hat{e}_x + \sin \phi_q \hat{e}_y)$, and the impact parameter $\mathbf{b}_\perp = b(\cos \phi_b \hat{e}_x + \sin \phi_b \hat{e}_y)$ denotes the position in the transverse plane from the center of momentum (*c.m.*) of the deuteron. For $\lambda = \pm 1$ or $\lambda = 0$, there are two independent helicity conserving form factors G_{11}^+ and G_{00}^+ which can be expressed in terms of $G_{C,M,Q}$ as [115],

$$G_{11}^+ = \frac{1}{1+\eta} \left\{ G_C + \eta G_M + \frac{\eta}{3} G_Q \right\}, \quad (17)$$

$$G_{00}^+ = \frac{1}{1+\eta} \left\{ (1-\eta) G_C + 2\eta G_M - \frac{2\eta}{3} (1+2\eta) G_Q \right\}, \quad (18)$$

with $\eta \equiv Q^2/(4M_d^2)$, and M_d is the deuteron mass. Using the formulas of G_C , G_M and G_Q in terms of $F(Q^2)$ in the soft-wall AdS/QCD model, one can rewrite the expression of the helicity conserving form factors as

$$G_{11}^+ = \{1 + \eta c_3\} F(Q^2), \quad (19)$$

$$G_{00}^+ = \left\{ \frac{1-\eta-2\eta^2}{1+\eta} + 2\eta c_2 - 2\eta^2 c_3 \right\} F(Q^2). \quad (20)$$

In Fig.2-a and 2-b, we show the deuteron helicity conserving form factors G_{11}^+ and G_{00}^+ respectively evaluated in the soft-wall AdS/QCD model. In the same plots we compare the holographic results with the phenomenological parameterization of experimental data of deuteron form

factors [1]. One notices that G_{11}^+ and G_{00}^+ obtained in the AdS/QCD framework are in excellent agreement with the parameterization. The transverse charge densities for definite helicity i.e. longitudinally polarized deuterons are shown in Fig.3. Both the charge densities for $\lambda = 0$ (Fig.3-a) and $\lambda = 1$ (Fig.3-b) states are axially symmetric and they have the peak at *c.m.*.

The transverse charge densities for longitudinally polarized deuteron lead to the monopole pattern only. To get information about dipole and the quadrupole moments of the deuteron states, one needs to consider the charge densities for the transversely polarized deuteron. The transverse charge densities for the transversely polarized deuteron can be defined as,

$$\begin{aligned} \rho_{T s_\perp}^d(\mathbf{b}) &\equiv \int \frac{d^2 \mathbf{q}_\perp}{(2\pi)^2} e^{-i \mathbf{q}_\perp \cdot \mathbf{b}} \\ &\times \frac{1}{2P^+} \langle P^+, \frac{\mathbf{q}_\perp}{2}, s_\perp | J^+ | P^+, -\frac{\mathbf{q}_\perp}{2}, s_\perp \rangle, \end{aligned}$$

where s_\perp is the deuteron spin projection along the transverse polarization direction, $\mathbf{S}_\perp = \cos \phi_S \hat{e}_x + \sin \phi_S \hat{e}_y$. For $s_\perp = +1$ and $s_\perp = 0$, the charge densities are given by [115],

$$\begin{aligned} \rho_{T 1}^d(\mathbf{b}) &= \int_0^\infty \frac{dQ}{2\pi} Q \left\{ J_0(bQ) \frac{1}{2} (G_{11}^+ + G_{00}^+) \right. \\ &\quad \left. + \sin(\phi_b - \phi_S) J_1(bQ) \sqrt{2} G_{01}^+ \right. \\ &\quad \left. - \cos 2(\phi_b - \phi_S) J_2(bQ) \frac{1}{2} G_{-1+1}^+ \right\}, \end{aligned} \quad (21)$$

$$\begin{aligned} \rho_{T 0}^d(\mathbf{b}) &= \int_0^\infty \frac{dQ}{2\pi} Q \left\{ J_0(bQ) G_{11}^+ \right. \\ &\quad \left. + \cos 2(\phi_b - \phi_S) J_2(bQ) G_{-1+1}^+ \right\}. \end{aligned} \quad (22)$$

It can be noticed that $\rho_{T 1}^d$ is a linear combination of helicity conserving charge densities together with two other components. The second term involves one unit of light-front helicity flip ($0 \rightarrow 1$) deuteron form factor which gives a dipole field pattern in the charge density. The last term in $\rho_{T 1}^d$, involves the form factor with two unit of helicity flip ($-1 \rightarrow +1$) and corresponds to a quadrupole field pattern in the charge density. But $\rho_{T 0}^d$ does not contain the dipole field pattern. One writes the deuteron form factor with one unit of helicity flip in terms of $G_{C,M,Q}$ as [115],

$$G_{01}^+ = -\frac{\sqrt{2\eta}}{1+\eta} \left\{ G_C - \frac{1}{2} (1-\eta) G_M + \frac{\eta}{3} G_Q \right\}, \quad (23)$$

whereas the deuteron form factor with two units of helicity flip, which governs the quadrupole field patterns is given by,

$$G_{-1+1}^+ = \frac{\eta}{1+\eta} \left\{ G_C - G_M - (1 + \frac{2\eta}{3}) G_Q \right\}. \quad (24)$$

In the soft-wall AdS/QCD model the deuteron helicity form factors with one and two units of helicity flip, can be

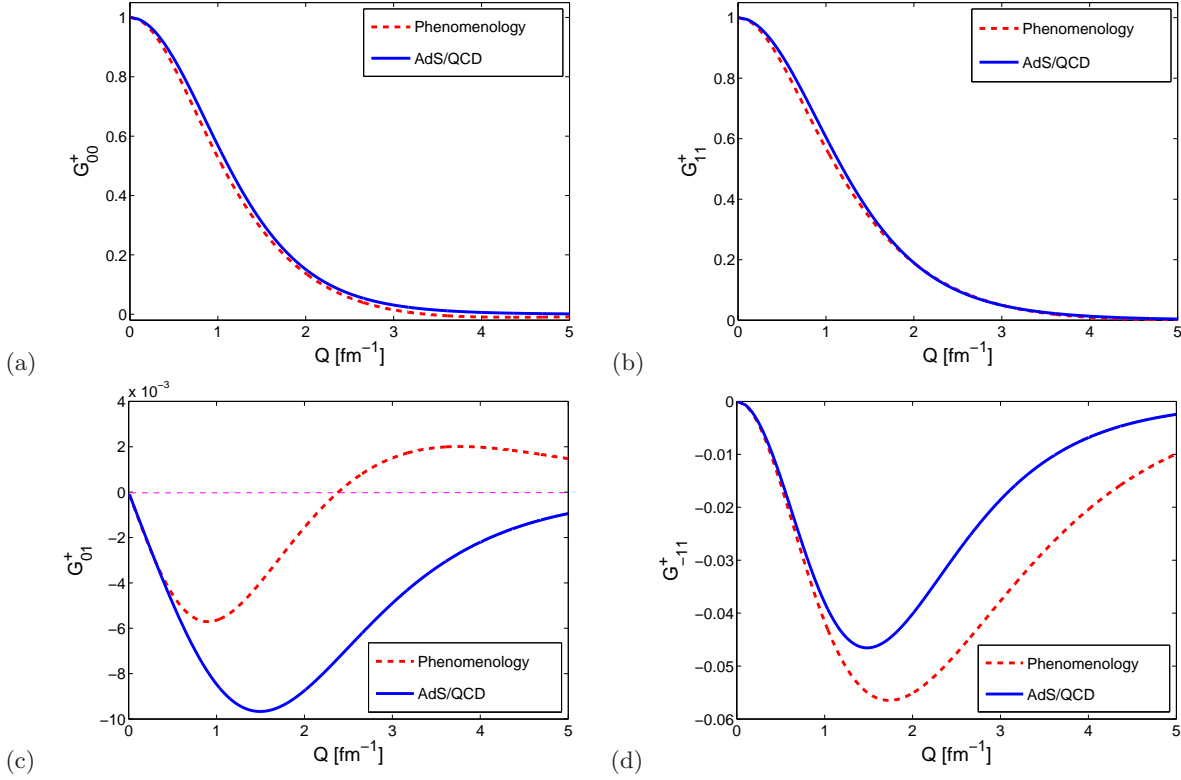


Fig. 2. (Color online) Deuteron helicity-conserving form factors (a) $G_{00}^+(Q^2)$, (b) $G_{11}^+(Q^2)$ and helicity-flip form factors (c) with one unit of helicity-flip: $G_{01}^+(Q^2)$ (a factor of 10^{-3} is taken out in the y -axis), (d) with two unit of helicity-flip: $G_{-11}^+(Q^2)$ are plotted against Q . The red dashed line represents the phenomenological parameterization of the deuteron form factors data [1] and the solid blue line represents the results of soft-wall AdS/QCD.

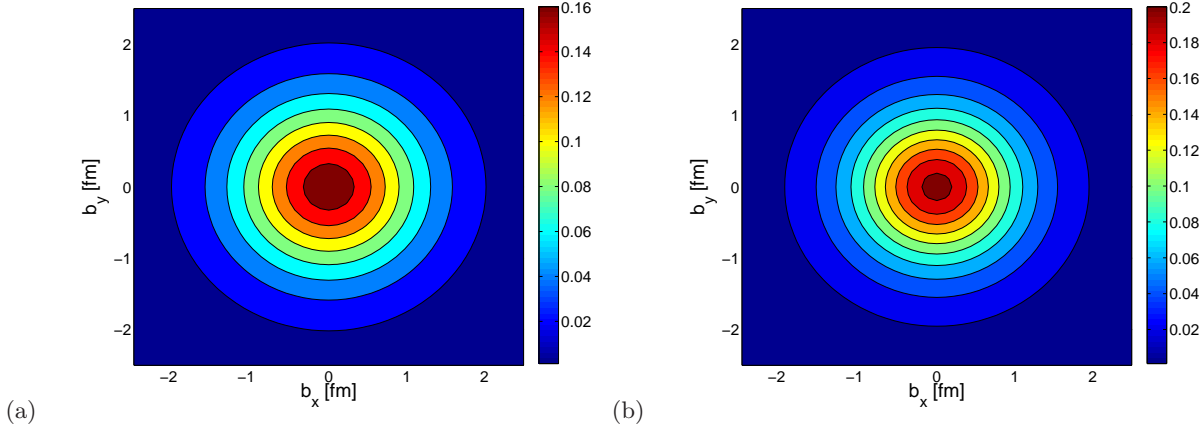


Fig. 3. (Color online) Top view of the three-dimensional quark transverse charge densities in the deuteron evaluated in AdS/QCD: (a) ρ_0^d and (b) ρ_1^d are for the longitudinally polarized deuterons.

expressed in terms of $F(Q^2)$ as,

$$G_{01}^+ = -\sqrt{2\eta} \left\{ 1 - \frac{c_2}{2} + \eta c_3 \right\} F(Q^2), \quad (25)$$

$$G_{-1+1}^+ = -\eta c_3 F(Q^2). \quad (26)$$

We show the deuteron helicity flip form factors, G_{01}^+ and G_{-1+1}^+ calculated in AdS/QCD framework in Fig.2-c and Fig.2-d, respectively. It can be noticed that though the

deuteron helicity conserving form factors in the AdS/QCD agree well with the phenomenological parameterization, the helicity flip form factors deviate at higher values of Q . Since η is very small within the range of Q^2 in the plots, for the spin non-flip form factors (Eqs.17 and 18) the only dominating contribution is coming from G_C which is in very good agreement with phenomenology (see Fig.1-a), G_M and G_Q are suppressed by η . Thus, the spin conserv-

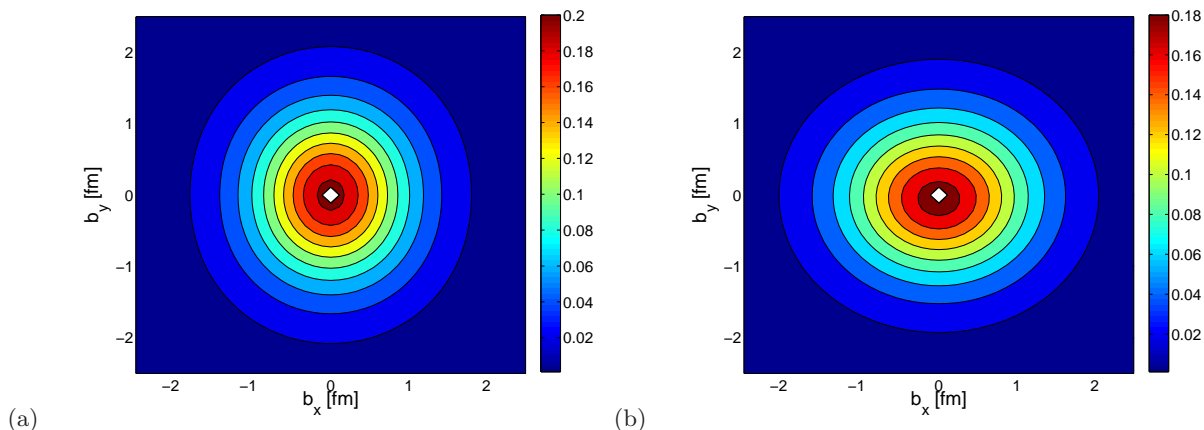


Fig. 4. (Color online) Top view of the three-dimensional quark transverse charge densities in the transversely polarized deuteron evaluated in AdS/QCD: (a) ρ_{T0}^d and (b) ρ_{T1}^d are for the deuteron which is transversely polarized along the positive x -axis.

ing form factors agree well with the phenomenological parameterization. But for spin-flip form factor G_{01}^+ (Eq.23), the major contributions are coming from G_C , and G_M (G_Q is suppressed by η) with a relative negative sign which causes the small magnitude of G_{01}^+ (of the order of 10^{-3}) but the errors add up as can be seen from Fig.1. A similar reason is also applicable for the mismatch in G_{-1+1}^+ .

The AdS/QCD results for the transverse charge density with transverse deuteron polarization are shown in Fig.4. Fig.4-a shows the charge distribution for the state with spin projection-0 in the x -direction whereas Fig.4-b exhibits charge density for a state with spin projection-1 in the x -direction. One finds that the effects of the quadrupole term in ρ_{T0}^d stretches the charge along the y -axis but does not cause any shift of the charge center whereas the quadrupole term in ρ_{T1}^d stretches the charge along the x -axis and the dipole term causes a small overall shift of the charge distribution along the y -axis. We show the individual monopole and quadrupole contributions to the charge density, ρ_{T0}^d in Fig.5 and the monopole, dipole, and quadrupole contributions to ρ_{T1}^d in Fig.6. The dipolar and quadrupole patterns come in the densities due to the small anomalous magnetic moment coming from the second term of the Eq.(21) which produces an induced electric dipole moment in y -direction and the anomalous electric quadrupole moment coming from the third term of the Eq.(21). It can be noted that the signs of quadrupole contributions to the charge densities are opposite, thus, the stretching of ρ_{T0}^d is along the y -axis but for ρ_{T1}^d , it is along the x -axis. The dipole or quadrupole contributions to the charge densities are comparatively very weak with respect to the monopole contributions. A comparison of the deuteron charge densities evaluated in soft-wall the AdS/QCD model and the phenomenological results [115] obtained using the parameterization of the experimental data for the deuteron electromagnetic form factors [1] are shown in Fig.7. We find that the AdS/QCD predictions for ρ_1^d and ρ_{T0}^d are in good agreement with the phenomenological results except at $b = 0$. The dip appearing at $b = 0$ in Fig.7(a) might be an artifact of the parameterization

of the phenomenological data. Again, the holographic prediction shows the overall small shift of ρ_{T1}^d from the *c.m.* in opposite direction to the phenomenological result. The shifting in ρ_{T1}^d occurs due to the dipole contribution which is coming from the one unit of light-front helicity flip ($0 \rightarrow 1$) deuteron form factor, $G_{01}^+(Q^2)$. It can be noticed that the phenomenological parameterization for $G_{01}^+(Q^2)$ shows a positive value after $Q \sim 2.3 \text{ fm}^{-1}$, however, it is always negative in the holographic QCD model (Fig.2-c). This produces the opposite shift in ρ_{T1}^d in the AdS/QCD model from the phenomenological result.

4 Generalized parton distributions for the deuteron

Generalized parton distributions encode the information about the three dimensional spatial structure of the hadron as well as the spin and orbital angular momentum of the constituents. GPDs are defined through the matrix element of the QCD non-local and non-diagonal operators on the light-front. For the deuteron (spin-1 particle), there are five vector GPDs which are defined by [51]

$$\begin{aligned}
 & \int \frac{p^+ dy^-}{2\pi} e^{ixp^+ y^-} \langle p_2, \lambda_2 | \bar{q}(-\frac{y}{2}) \gamma^+ q(\frac{y}{2}) | p_1, \lambda_1 \rangle_{y^+ = y_\perp = 0} \\
 &= -2(\varepsilon_2^* \cdot \varepsilon_1) p^+ H_1 - (\varepsilon_1^+ \varepsilon_2^* \cdot q - \varepsilon_2^{+*} \varepsilon_1 \cdot q) H_2 \\
 &+ q \cdot \varepsilon_1 q \cdot \varepsilon_2^* \frac{p^+}{m_n^2} H_3 - (\varepsilon_1^+ \varepsilon_2^* \cdot q + \varepsilon_2^{+*} \varepsilon_1 \cdot q) H_4 \\
 &+ \left(\frac{m_n^2}{(p^+)^2} \varepsilon_1^+ \varepsilon_2^{+*} + \frac{1}{3} (\varepsilon_2^* \cdot \varepsilon_1) \right) 2p^+ H_5. \quad (27)
 \end{aligned}$$

All the GPDs are functions of the three variables namely, the longitudinal momentum fraction x carried by the active quark, the square of the total momentum transferred t and the fraction of the longitudinal momentum transferred ξ , the so called skewness. In symmetric frame the kinematical variables are $p^\mu = \frac{(p+p')^\mu}{2}$, $q^\mu = p'^\mu - p^\mu$, $\xi = -\frac{q^+}{2P^+}$,

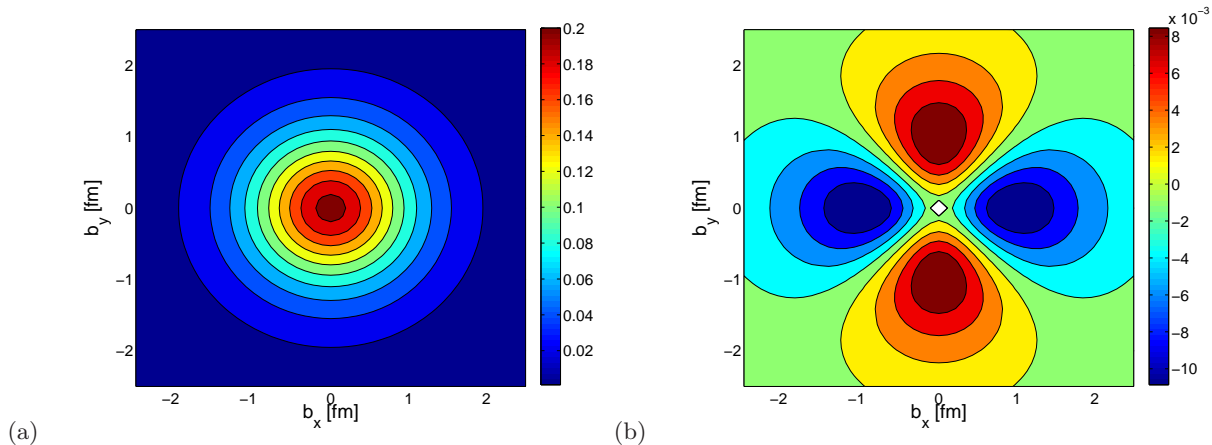


Fig. 5. (Color online) (a) Monopole and (b) quadrupole contributions to the charge density: ρ_{T0}^d .

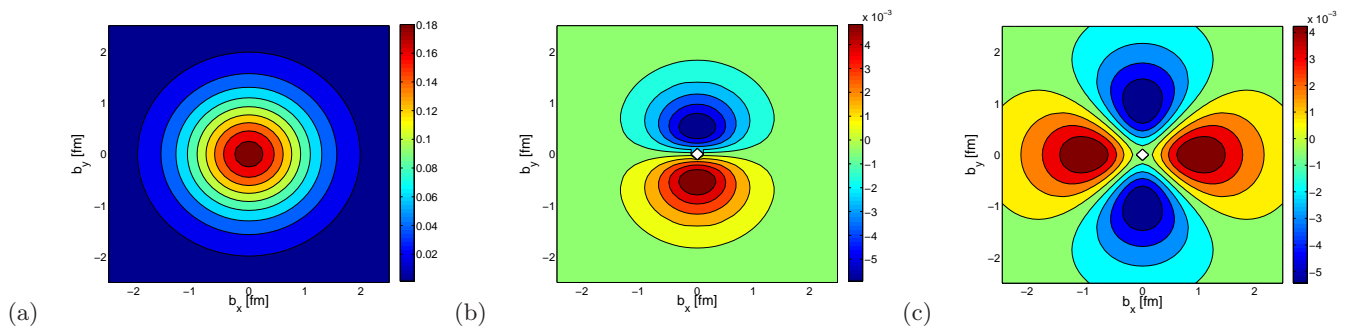


Fig. 6. (Color online) (a) Monopole, (b) dipole and (c) quadrupole contributions to the charge density: ρ_{T1}^d .

and $t = q^2$. The first moments of GPDs are related to the form factors of the deuteron by

$$\int_0^1 dx H_v^i(x, \xi, t) = G_i(t), \quad i = 1, 2, 3 \quad (28)$$

$$\int_0^1 dx H_v^i(x, \xi, t) = 0, \quad i = 4, 5, \quad (29)$$

where the GPDs for the valence quark are defined as $H_v^i(x, 0, t) = H^i(x, 0, t) + H^i(-x, 0, t)$. Using the integral representation of $V(z, Q^2)$ in Eq. (13), one can rewrite the deuteron form factors in Eqs. (10,11) as

$$G_i(Q^2) = c_i \int_0^1 dx \int_0^\infty dz \frac{\kappa^{12} z^{11}}{12} \frac{x^{Q^2}}{(1-x)^2} e^{-\frac{\kappa^2 z^2}{(1-x)}}. \quad (30)$$

Comparing the integrands in Eqs. (28) and (30), we extract the GPDs for the deuteron in the following forms:

$$H_v^i(x, 0, Q^2) = c_i \int_0^\infty dz \frac{\kappa^{12} z^{11}}{12} \frac{x^{Q^2}}{(1-x)^2} e^{-\frac{\kappa^2 z^2}{(1-x)}}, \quad (31)$$

where $t = -Q^2$, and $c_1 = 1$, $c_2 = 1.714$, and $c_3 = 26.544$ [48]. Here we evaluate the deuteron GPDs when the skewness is zero ($\xi = 0$). Since the GPD $H^4(x, \xi, t)$ is odd in ξ , H^4 is zero for $\xi = 0$ [51]. But the other GPDs are even

in ξ . In Fig. 8, we show the deuteron GPD $H_v^1(x, 0, Q^2)$ as a function of x and Q^2 . The GPD has a peak at very low momentum fraction x , and also when the momentum transfer is low but the value decreases and goes to zero with increasing x and Q^2 . The other GPDs can be obtained by multiplying the constant c_i with $H_v^1(x, 0, Q^2)$.

5 Longitudinal momentum densities in the transverse plane for the deuteron

Similar to the electromagnetic densities, we can identify the gravitomagnetic density (p^+ momentum density) in the transverse plane by taking the Fourier transform of the gravitational form factor [104, 116]. Thus, the longitudinal momentum (p^+) density for the deuteron can be defined as

$$\rho_\lambda^+(\mathbf{b}_\perp) = \int \frac{d^2 \mathbf{q}_\perp}{(2\pi)^2} e^{-i\mathbf{q}_\perp \cdot \mathbf{b}} \mathcal{T}_{\lambda\lambda}^+(Q^2), \quad (32)$$

where the form factor $\mathcal{T}_{\lambda\lambda}^+(Q^2)$ is given by the matrix elements of the stress tensor

$$\begin{aligned} & \left\langle p^+, \frac{\mathbf{q}_\perp}{2}, \lambda_2 \left| T^{++}(0) \right| p^+, -\frac{\mathbf{q}_\perp}{2}, \lambda_1 \right\rangle \\ & = 2(p^+)^2 e^{i(\lambda_1 - \lambda_2)\phi_q} \mathcal{T}_{\lambda_2 \lambda_1}^+(Q^2). \end{aligned} \quad (33)$$

For spin-1 particles, there are two independent helicity conserving form factors \mathcal{T}_{11}^+ , and \mathcal{T}_{00}^+ which are given by

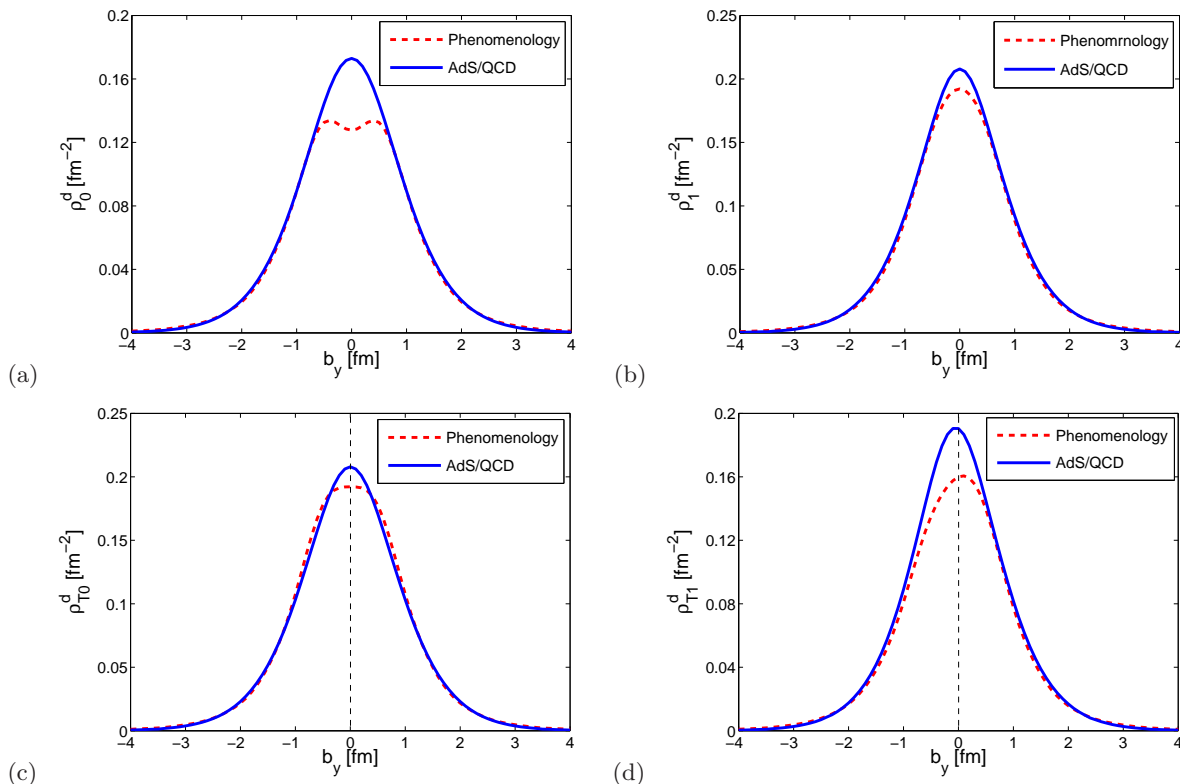


Fig. 7. (Color online) Comparison of transverse charge densities in the deuteron evaluated in AdS/QCD and the phenomenological results: (a) ρ_0^d and (b) ρ_1^d are for the longitudinally polarized deuterons (c) ρ_{T0}^d and (d) ρ_{T1}^d are for the deuteron which is transversely polarized along the positive x -axis. The solid blue and red dashed lines represent the results of AdS/QCD and the phenomenological results [115] respectively.

[116, 53]

$$\begin{aligned} \mathcal{T}_{00}^+(Q^2) &= Z_1(Q^2) = \int dz \mathcal{H}(Q, z) \partial_z \Phi_0(z) \partial_z \Phi_0(z), \\ \mathcal{T}_{11}^+(Q^2) &= Z_2(Q^2) = \int dz \mathcal{H}(Q, z) \Phi_0(z) \Phi_0(z), \end{aligned} \quad (34)$$

where the form of the profile function $\mathcal{H}(Q, z)$ in the soft-wall AdS/QCD model is [116, 60]

$$\mathcal{H}(Q, z) = \Gamma(4\eta + 2) U(4\eta, -1, z^2), \quad (35)$$

where $U(a, b, w)$ is the 2nd Kummer function and $\Phi_0(z)$ is the normalizable wave function, $\int dz \Phi_0^2 = 1$. We use the deuteron wave function (Eq.(8)) in Eq.(34) to evaluate the gravitational form factors $Z_1(Q^2)$ and $Z_2(Q^2)$. Now, one can obtain the p^+ densities as

$$\begin{aligned} \rho_1^+(\mathbf{b}_\perp) &= \int_0^\infty \frac{dQ}{2\pi} Q J_0(bQ) Z_2(Q^2), \\ \rho_0^+(\mathbf{b}_\perp) &= \int_0^\infty \frac{dQ}{2\pi} Q J_0(bQ) Z_1(Q^2). \end{aligned} \quad (36)$$

We show the helicity conserving gravitational form factors \mathcal{T}_{00}^+ and \mathcal{T}_{11}^+ as a function of Q^2 in Fig. 9(a). One can notice that at $Q^2 = 0$, $\mathcal{T}_{\lambda, \lambda}^+ = 1$. Thus, it follows the momentum sum rule. The longitudinal momentum densities in the

transverse plane are shown in Fig. 9(b). We observe that both the densities ρ_1^+ and ρ_0^+ are more or less same in the transverse plane.

6 Summary

In this work, we have studied the transverse charge densities in longitudinally and transversely polarized deuterons using the empirical formulae of the deuteron electromagnetic form factors evaluated in the framework of the soft-wall AdS/QCD. We found that the charge densities for longitudinally polarized deuterons are axially symmetric and exhibit the monopole pattern only. Transversely polarized deuterons show a monopole pattern together with the dipole and quadrupole structure in the charge distributions. The dipolar structure which appears only in the distribution for the transversely polarized deuteron state with spin projection $s_\perp = 1$ causes a small overall shift in ρ_{T1}^d along the y -axis. The quadrupole structures stretch the charge distributions along the y -axis or x -axis but does not cause any shift from the $c.m.$. The monopole contributions to the charge densities are large compared to the dipole and quadrupole. Further, we have compared the AdS/QCD results with the consequences of phenomenological parameterization [115]. Except for the mismatch in ρ_0^d at the center and the overall small shift in ρ_{T1}^d which

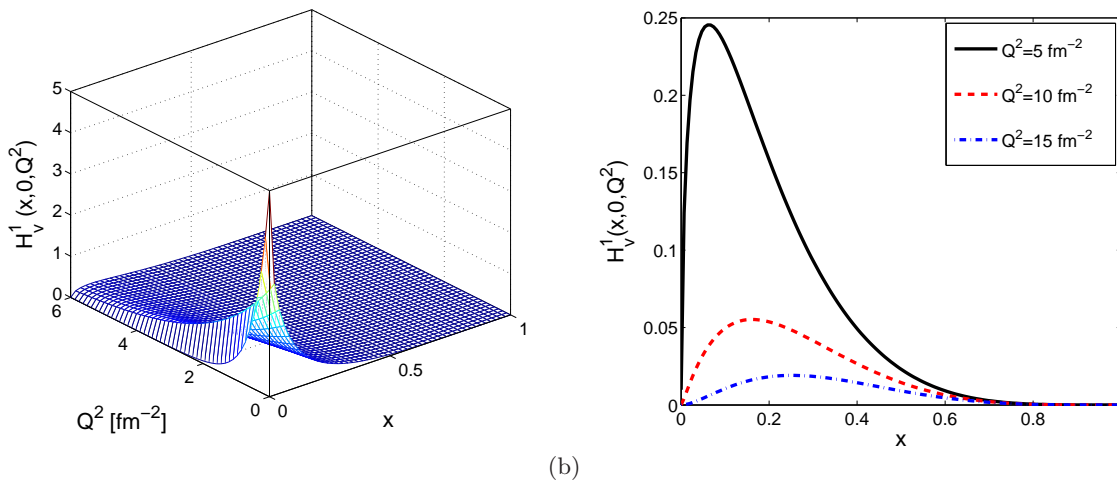


Fig. 8. (Color online) Plot of the deuteron GPD $H_V^1(x, 0, Q^2)$ as a function of x and Q^2 . The other GPDs are $H_V^i(x, 0, Q^2) = c_i H_V^1(x, 0, Q^2)$, $i = 2, 3$ where $c_2 = 1.714$, and $c_3 = 26.544$.

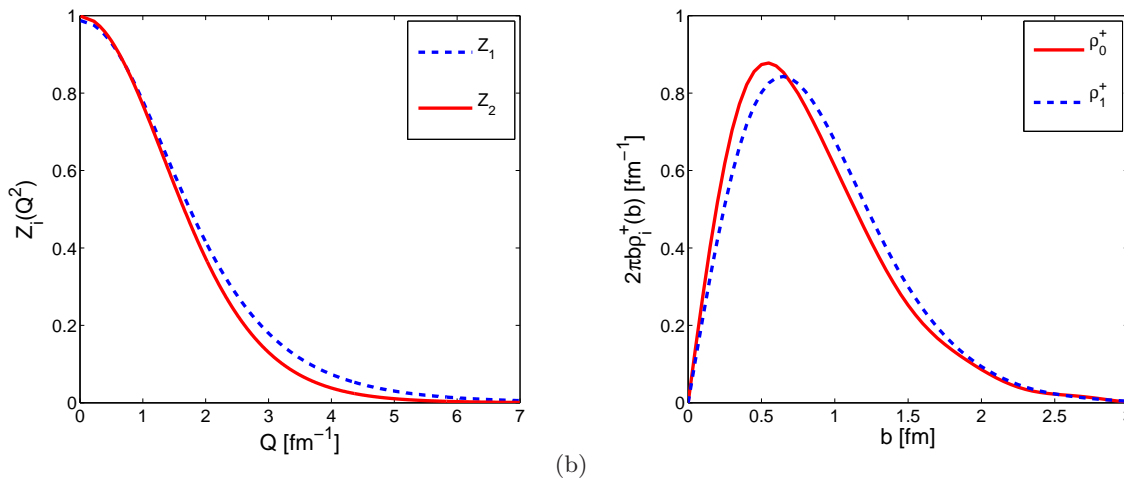


Fig. 9. (Color online) Plots of (a) gravitational form factors for the deuteron, and (b) Longitudinal momentum densities in the deuteron.

is opposite to phenomenological result, the comparison shows that the AdS/QCD predictions are in reasonable agreement with the phenomenological parameterization.

Then we have shown the GPDs for the deuteron obtained from the electromagnetic form factors using the integral representation form of the bulk to boundary propagator and the GPDs sum rule. We have also evaluated the helicity non-flip gravitational form factors and shown that they satisfy the physical condition at $Q^2 = 0$. Finally, the longitudinal momentum densities in the transverse plane have been investigated and we found that the longitudinal momentum densities are independent of the deuteron helicity.

This work is supported by new faculty startup funding by the Institute of Modern Physics, Chinese Academy of Sciences under the Grand No. Y632030YRC.

References

1. D. Abbott *et al.* (JLAB t20 Collaboration), *Eur. Phys. J. A* **7**, 421 (2000).
2. M. Garcon and J. W. Van Orden, *Adv. Nucl. Phys.* **26**, 293 (2001).
3. M. Kohl, *Nucl. Phys. A* **805**, 361 (2008).
4. R. J. Holt and R. Gilman, *Rep. Prog. Phys.* **75**, 086301 (2012).
5. C. D. Buchanan and M. R. Yearian, *Phys. Rev. Lett.* **15**, 303 (1965).
6. J. E. Elias, J. I. Friedman, G. C. Hartmann, H. W. Kendall, P. N. Kirk, M. R. Sogard, L. P. Van Speybroeck and J. K. De Pagter, *Phys. Rev.* **177**, 2075 (1969).
7. D. Benaksas, D. Drickey and D. Frerejacque, *Phys. Rev. Lett.* **13**, no. 10, 353 (1964).
8. D. Benaksas, D. Drickey and D. Frerejacque, *Phys. Rev.* **148**, 1327 (1966).
9. S. Platchkov *et al.*, *Nucl. Phys. A* **510**, 740 (1990).
10. S. Galster, H. Klein, J. Moritz, K. H. Schmidt, D. Wegener and J. Bleckwenn, *Nucl. Phys. B* **32**, 221 (1971).

11. R. Cramer *et al.*, *Z. Phys. C* **29**, 513 (1985).
12. G. G. Simon, C. Schmitt and V. H. Walther, *Nucl. Phys. A* **364**, 285 (1981).
13. D. Abbott *et al.* [Jefferson Lab t(20) Collaboration], *Phys. Rev. Lett.* **82**, 1379 (1999).
14. R. W. Berard, F. R. Buskirk, E. B. Dally, J. N. Dyer, X. K. Maruyama, R. L. Topping and T. J. Traverso, *Phys. Lett.* **47B**, 355 (1973).
15. P. E. Bosted *et al.*, *Phys. Rev. C* **42**, 38 (1990).
16. S. Auffret *et al.*, *Phys. Rev. Lett.* **54**, 649 (1985).
17. R. G. Arnold *et al.*, *Phys. Rev. Lett.* **58**, 1723 (1987).
18. M. E. Schulze *et al.*, *Phys. Rev. Lett.* **52**, 597 (1984).
19. M. Garcon *et al.*, *Phys. Rev. C* **49**, 2516 (1994).
20. I. The *et al.*, *Phys. Rev. Lett.* **67**, 173 (1991).
21. D. Abbott *et al.* [JLAB t(20) Collaboration], *Phys. Rev. Lett.* **84**, 5053 (2000).
22. V. F. Dmitriev *et al.*, *Phys. Lett.* **157B**, 143 (1985).
23. R. A. Gilman *et al.*, *Phys. Rev. Lett.* **65**, 1733 (1990).
24. M. Ferro-Luzzi *et al.*, *Phys. Rev. Lett.* **77**, 2630 (1996).
25. M. Bouwhuis *et al.*, *Phys. Rev. Lett.* **82**, 3755 (1999).
26. D. M. Nikolenko *et al.*, *Phys. Rev. Lett.* **90**, 072501 (2003).
27. C. Zhang *et al.*, *Phys. Rev. Lett.* **107**, 252501 (2011).
28. S. J. Brodsky, C. R. Ji, and G. P. Lepage, *Phys. Rev. Lett.* **51**, 83 (1983).
29. F. M. Lev, E. Pace, and G. Salme, *Phys. Rev. Lett.* **83**, 5250 (1999).
30. R. G. Arnold, C. E. Carlson, and F. Gross, *Phys. Rev. C* **21**, 1426 (1980).
31. R. G. Arnold, C. E. Carlson, and F. Gross, *Phys. Rev. C* **23**, 363 (1981).
32. T. De Forest, Jr. and J. D. Walecka, *Adv. Phys.* **15**, 1 (1966).
33. A. A. Logunov and A. N. Tavkhelidze, *Nuovo Cim.* **29**, 380 (1963).
34. T. W. Donnelly and J. D. Walecka, *Ann. Rev. Nucl. Part. Sci.* **25**, 329 (1975).
35. J. L. Friar, *Phys. Rev. C* **12**, 695 (1975).
36. J. F. Mathiot, *Phys. Rept.* **173**, 63 (1989).
37. R. Schiavilla and D. O. Riska, *Phys. Rev. C* **43**, 437 (1991).
38. T. W. Allen, G. L. Payne, and W. N. Polyzou, *Phys. Rev. C* **62**, 054002 (2000).
39. R. Blankenbecler and R. Sugar, *Phys. Rev.* **142**, 1051 (1966).
40. W. W. Buck and F. Gross, *Phys. Rev. D* **20**, 2361 (1979).
41. J. Carbonell, B. Desplanques, V. A. Karmanov, and J. F. Mathiot, *Phys. Rep.* **300**, 215 (1998).
42. V. A. Karmanov and A. V. Smirnov, *Nucl. Phys. A* **546**, 691 (1992).
43. S. Kolling, E. Epelbaum, and D. R. Phillips, *Phys. Rev. C* **86**, 047001 (2012).
44. E. Epelbaum, A. M. Gasparyan, J. Gegelia, and M. R. Schindler, *Eur. Phys. J. A* **50**, 51 (2014).
45. A. Buchmann, Y. Yamauchi, and A. Faessler, *Phys. Lett. B* **225**, 301 (1989).
46. H. Ito and L. S. Kisslinger, *Phys. Rev. C* **40**, 887 (1989).
47. Y. B. Dong, A. Faessler, T. Gutsche, and V. E. Lyubovitskij, *Phys. Rev. C* **78**, 035205 (2008).
48. T. Gutsche, V. E. Lyubovitskij, I. Schmidt and A. Vega, *Phys. Rev. D* **91**, no. 11, 114001 (2015).
49. T. Gutsche, V. E. Lyubovitskij and I. Schmidt, *Phys. Rev. D* **94**, no. 11, 116006 (2016).
50. V. E. Lyubovitskij, T. Gutsche, I. Schmidt and A. Vega, *Few Body Syst.* **57**, no. 7, 503 (2016).
51. E. R. Berger, F. Cano, M. Diehl and B. Pire, *Phys. Rev. Lett.* **87**, 142302 (2001).
52. Y. Dong and C. Liang, *J. Phys. G* **40**, 025001 (2013).
53. Z. Abidin and C. E. Carlson, *Phys. Rev. D* **77**, 095007 (2008).
54. S. J. Brodsky and G. F. de T eramond, *Phys. Lett. B* **582**, 211 (2004).
55. G. F. de Teramond and S. J. Brodsky, *AIP Conf. Proc.* **1296**, 128 (2010) doi:10.1063/1.3523157 [arXiv:1006.2431 [hep-ph]].
56. S. J. Brodsky and G. F. de T eramond, *Phys. Rev. Lett.* **96**, 201601 (2006).
57. S. J. Brodsky and G. F. de T eramond, *Phys. Rev. D* **77**, 056007 (2008).
58. J. Erlich, E. Katz, D. T. Son and M. A. Stephanov, *Phys. Rev. Lett.* **95**, 261602 (2005).
59. T. Sakai and S. Sugimoto, *Prog. Theo. Phys.* **113**, 843 (2005).
60. Z. Abidin and C. E. Carlson, *Phys. Rev. D* **79**, 115003 (2009).
61. H. Forkel, M. Beyer and T. Frederico, *Int. J. Mod. Phys. E* **16**, 2794 (2007).
62. W. de Paula, T. Frederico, H. Forkel and M. Beyer, *Phys. Rev. D* **79**, 075019 (2009).
63. A. Vega, I. Schimdt, T. Gutsche and V. E. Lyubovitskij, *Phys. Rev. D* **83**, 036001 (2011).
64. A. Vega, I. Schimdt, T. Gutsche and V. E. Lyubovitskij, *Phys. Rev. D* **85**, 096004 (2012).
65. T. Gutsche, V. E. Lyubovitskij, I. Schmidt and A. Vega, *Phys. Rev. D* **86**, 036007 (2012).
66. S. J. Brodsky and G. F. de T eramond, *Phys. Rev. D* **78**, 025032 (2008).
67. H. R. Grigoryan and A. V. Radyushkin, *Phys. Rev. D* **76**, 095007 (2007).
68. S. J. Brodsky and G. F. de T eramond, arXiv:1203.4025 [hep-ph].
69. G. F. de Teramond and S. J. Brodsky, *Phys. Rev. Lett.* **94**, 201601 (2005).
70. A. Vega, I. Schmidt, T. Branz, T. Gutsche, V. E. Lyubovitskij, *Phys. Rev. D* **80**, 055014 (2009).
71. T. Branz, T. Gutsche, V. E. Lyubovitskij, I. Schmidt and A. Vega, *Phys. Rev. D* **82**, 074022 (2010).
72. D. Chakrabarti and C. Mondal, *Phys. Rev. D* **88**, 073006 (2013).
73. D. Chakrabarti and C. Mondal, *Eur. Phys. J. C* **73**, 2671 (2013).
74. D. Chakrabarti and C. Mondal, *Eur. Phys. J. C* **74**, 2962 (2014).
75. K. Hashimoto, T. Sakai and S. Sugimoto, *Prog. Theor. Phys.* **120**, 1093 (2008).
76. C. Mondal, *Eur. Phys. J. C* **76**, 74 (2016).
77. T. Liu and B. Q. Ma, *Phys. Rev. D* **92**, 096003 (2015).
78. T. Gutsche, V. E. Lyubovitskij, I. Schmidt and A. Vega, *Phys. Rev. D* **87**, 016017 (2013).
79. D. Chakrabarti and C. Mondal, *Eur. Phys. J. A* **52**, no. 9, 285 (2016).
80. G. F. de Teramond and S. J. Brodsky, *AIP Conf. Proc.* **1432**, 168 (2012).
81. G. F. de Teramond, H. G. Dosch and S. J. Brodsky, *Phys. Rev. D* **91**, 045040 (2015).
82. H. G. Dosch, G. F. de Teramond and S. J. Brodsky, *Phys. Rev. D* **91**, 085016 (2015).

83. S. J. Brodsky, G. F. de Teramond, H. G. Dosch and J. Erlich, *Phys. Rept.* **584**, 1 (2015).
84. G. F. de Teramond, H. G. Dosch and S. J. Brodsky, *Phys. Rev. D* **87**, no. 7, 075005 (2013).
85. R. S. Sufian, G. F. de Tramond, S. J. Brodsky, A. Deur and H. G. Dosch, *Phys. Rev. D* **95**, no. 1, 014011 (2017).
86. Y. Kim, C. H. Lee, and H. U. Yee, *Phys. Rev. D* **77**, 085030 (2008).
87. O. Aharony, K. Peeters, J. Sonnenschein, and M. Zamaklar, *JHEP* **02**, 071 (2008).
88. Y. Kim, Y. Seo, and S. J. Sin, *JHEP* **03**, 074 (2010).
89. O. Bergman, G. Lifschytz, and M. Lippert, *JHEP* **11**, 056 (2007).
90. M. Rozali, H. H. Shieh, M. Van Raamsdonk, and J. Wu, *JHEP* **01**, 053 (2008).
91. K. Hashimoto, *Prog. Theor. Phys.* **121**, 241 (2009).
92. M. Harada, S. Nakamura, and S. Takemoto, *Phys. Rev. D* **86**, 021901 (2012).
93. Y. Kim and D. Yi, *Adv. High Energy Phys.* **2011**, 259025 (2011).
94. S. Aoki, K. Hashimoto, and N. Iizuka, *Rep. Prog. Phys.* **76**, 104301 (2013).
95. Y. Kim, I. J. Shin, and T. Tsukioka, *Prog. Part. Nucl. Phys.* **68**, 55 (2013).
96. M. R. Pahlavani and R. Morad, *Adv. High Energy Phys.* **2014**, 863268 (2014).
97. M. Burkardt, *Phys. Rev. D* **62**, 071503 (2000).
98. M. Burkardt, *Int. J. Mod. Phys. A* **18**, 173 (2003).
99. G. A. Miller, *Phys. Rev. C* **80**, 045201 (2009).
100. G. A. Miler, *Annu. Rec. Part. Sci.* **60**, 1 (2010).
101. S. Venkat, J. Arrington, G. A. Miller and X. Zhan, *Phys. Rev. C* **83**, 015203 (2011).
102. G. A. Miller, *Phys. Rev. Lett.* **99**, 112001 (2007).
103. C. E. Carlson and M. Vanderhaeghen, *Phys. Rev. Lett.* **100**, 032004 (2008).
104. O.V. Selyugin and O.V. Teryaev, *Phys. Rev. D* **79**, 033003 (2009).
105. C. Mondal and D. Chakrabarti, *Eur. Phys. J. C* **75**, 261 (2015).
106. C. Mondal and D. Chakrabarti, *Few Body Syst.* **57**, no. 8, 723 (2016).
107. N. Sharma, *Phys. Rev. D* **90**, 095024 (2014).
108. C. Mondal, *Phys. Rev. D* **94**, no. 7, 073001 (2016).
109. C. Granados, C. Weiss, *JHEP* **1401**, 092 (2014).
110. D. S. Hwang, D. S. Kim and J. Kim, *Phys. Lett. B* **669**, 345 (2008).
111. N. Kumar and H. Dahiya, *Phys. Rev. D* **90**, no. 9, 094030 (2014).
112. C. Mondal, N. Kumar, H. Dahiya and D. Chakrabarti, *Phys. Rev. D* **94**, no. 7, 074028 (2016).
113. C. Liang, Y. Dong and W. Liang, *Commun. Theor. Phys.* **62**, no. 3, 383 (2014).
114. C. Liang, Y. Dong and W. Liang, *Chin. Phys. C* **38**, 074104 (2014).
115. C. E. Carlson and M. Vanderhaeghen, *Eur. Phys. J. A* **41**, 1 (2009).
116. Z. Abidin and C. E. Carlson, *Phys. Rev. D* **78**, 071502 (2008).
117. D. Chakrabarti, C. Mondal and A. Mukherjee, *Phys. Rev. D* **91**, 114026 (2015).
118. D. Chakrabarti, C. Mondal and A. Mukherjee, *Few Body Syst.* **57**, no. 6, 437 (2016).